A HicA toxin-based counter-selection marker for allelic exchange mutations in *Fusobacterium nucleatum*

Bibek GC, Peng Zhou and Chenggang Wu[†]

Department of Microbiology & Molecular Genetics, the University of Texas Health Science Center, Houston, TX, USA

[†] To whom correspondence should be addressed. Tel. (+1) 713 500 5437; E-mail: chenggang.wu@uth.tmc.edu

Running Title: HicA toxin as a counter-selection marker in *Fusobacterium nucleatum*

Keywords: HicA, toxin-antitoxin, counterselection marker, *Fusobacterium nucleatum*

ABSTRACT

The study of fusobacterial virulence factors has dramatically benefited from the creation of various genetic tools for DNA manipulation, including the *galK*-based counterselection for in-frame deletion mutagenesis in *Fusobacterium nucleatum* that we recently developed. However, this method requires a host lacking the GalK gene, which is an inherent limitation. To circumvent this limitation, we explored the possibility of using the HicA gene that encodes a toxin consisting of a HicAB toxin-antitoxin module in *Fusobacterium periodonticum* as a new counter-selective marker. Interestingly, the full-length HicA is not toxic in *F. nucleatum*, but a truncated HicA version lacking the first six amino acids is functional as a toxin. The toxin expression is driven by an *rpsJ* promoter and is controlled by its translational level using a theophylline-responsive riboswitch unit. As a proof of concept, we created markerless in-frame deletions in the fusobacterial adhesin RadD gene within *F. nucleatum rad* operon and the TnaA gene that encodes the tryptophanase for indole production. After vector integration, plasmid excision after counterselection appeared to have occurred in 100% of colonies grown on theophylline-added plates and resulted in in-frame deletions in 50% of the screened isolates. This HicA-based counterselection system provides a robust and reliable counterselection in wild-type background *F. nucleatum* and should also be adapted for use in other bacteria.

IMPORTANCE

Fusobacterium nucleatum is an indole-producing oral anaerobe associated with periodontal diseases, preterm birth, and several cancers. Little is known about the mechanisms of fusobacterial pathogenesis and associated factors mainly due to the lack of robust genetic tools for this organism. Here we showed that a mutated HicA gene from *Fuosbacerium periodonticum* expresses an active toxin and was used as a counterselection marker. This *hicA*-based in-frame deletion system efficiently creates in-frame deletion mutations in the wild-type background of *F. nucleatum*. This is the first report to use the *hicA* gene as a counterselection marker in a bacterial genetic study.

INTRODUCTION

42 *F. nucleatum* is a Gram-negative, indole-producing microorganism naturally isolated from
43 the oral cavity and is especially abundant within the subgingival plaque biofilm composed of
44 more than 400 bacterial species (1, 2). Using three major surface adhesin proteins, FadA (3, 4),
45 RadD (5, 6), and Fap2 (7, 8), *F. nucleatum* physically interacts with the host and many other
46 early or late colonizers in oral biofilm, making its presence tightly associated with the onset and
47 development of periodontal disease (2, 9, 10). In addition, evidence has shown that *F.*
48 *nucleatum* plays an essential role in extra-oral diseases like preterm birth (11, 12) and colorectal
49 cancer (13-16). To better understand the role of this bacterium in various disorders, it is
50 necessary to have comprehensive knowledge of *F. nucleatum's* biology and pathogenesis.
51 Such knowledge has been dramatically expanded in the past 15 years due to many genetic
52 tools being adapted for use in studies of this organism. There are two ways to perform genetic
53 studies of *F. nucleatum*. One way is to use the Tn5-based mutagenesis to produce many
54 random gene mutants in one single assay (7, 17); the other is to use the defined genetic
55 mutation that makes a single mutant each time. The defined mutations are usually engineered
56 using three methods: 1) plasmid insertion duplication mutagenesis (5, 18), 2) allelic exchange
57 mutagenesis with antibiotic cassette (3), and 3) markerless in-frame deletion (17, 19). The first
58 two methods are easy to carry out and were primarily employed in early studies of *F. nucleatum.*
59 But both have an obvious drawback, frequently creating undesirable polar effects on
60 downstream genes. One example is the early made *fadA* mutant strain (3). FadA is a major
61 adhesion/invasion factor that plays a significant role in the pathogenesis of *F. nucleatum* (4, 20).
62 This *fadA* mutation was generated by allelic exchange mutagenesis with erythromycin
63 resistance cassette *ermF-ermAM*. The generated mutant strain had a change in cell
64 morphology, which could not be restored with a *fadA* complementation (21). Interestingly, the
65 immediate downstream gene of *fadA* is *ftsX*, which encodes a cell division protein. Our previous
66 data (17) showed that FtsX is related to fusobacterial cytokinesis. So, it is possible that the

67 morphological alternation in this mutant strain was due to the erythromycin resistance cassette's
68 polar effect on *ftsX*. In addition, the number of available selectable markers limits the number of
69 mutations in a strain. However, these issues could be overcome by developing a markerless in-
70 frame deletion system.

71 The in-frame deletion procedure is a two-step process. First, two similarly sized fragments
72 that are homologous to sequences flanking the target locus are PCR amplified. The two
73 fragments are ligated adjacent to each other in a suicide vector. This construct is subsequently
74 integrated onto the chromosome via homologous recombination and selected using a positive
75 selection pressure, often with antibiotic resistance. Next, plasmid-excision/loss recombinants
76 are screened for a second recombination that occurs between the homologous regions, which is
77 created due to insertion duplication. Since the second recombination event is rare, screening
78 these recombinants that have undergone the double crossover is time-consuming.
79 Counterselection strategies are often introduced to facilitate this process to create markerless
80 in-frame deletions (22).

81 For this purpose, we introduced *galK* as a counterselection marker in *F. nucleatum* (17). The
82 *galK* gene encodes galactokinase, a key enzyme in galactose metabolism. This enzyme
83 phosphorylates D-galactose to generate galactose-1-phosphate and can also convert 2-deoxy-
84 D-galactose (2-DG) into 2-deoxygalctose-1-phosphate, which is not further metabolized and is
85 toxic to the cell. *F. nucleatum* carries a copy of the *galK* gene. To use *galK* for counterselection,
86 a *galK*-minus recipient strain must be constructed. An in-frame deletion vector was generated in
87 which the *galK* gene from *F. nucleatum* or *Clostridium acetobutylicum* was cloned, and a strong
88 and constitutive promoter controlled its expression. If the recipient strain lacks galactose kinase
89 (*galK*) and phosphate uridylyltransferase (*galT*), galactose could can be used instead of the
90 more expensive 2-deoxy-D-galactose molecule for selection (19). The *galK*-based
91 counterselection system consists of a *galK* minus or *galKT* recipient strain and an in-frame
92 deletion vector, which results in a strong negative selection in *F. nucleatum*. This shows that all

93 viable strains when selected with 2-deoxy-D-galactose undergo the second recombination to
94 excise the plasmid. This system successfully generated many fusobacterial in-frame deletions in
95 our lab and other groups (6, 17, 19, 23). However, the apparent limitation of this system is the
96 modified mutant recipient strain requirement. The intermediate product UDP-galactose from
97 galactose utilization is vital in cell envelope maintenance in bacteria (24, 25). The use of
98 galactose present in a culture medium or animal hosts by *F. nucleatum* could change its
99 physiology, as it would potentially module the function of Fap2, an important adhesin that binds
100 galactose and is responsible for cell-cell coaggregation and cell adhesion (7, 8). Consistently,
101 we identified several cases in which the recipient background impacted the phenotypes of our
102 markerless in-frame deletion strains in our studies (unpublished data). Thus, a new
103 counterselection marker is urgently needed to replace *galK* for genetic studies in *F. nucleatum*.
104 The HicAB is a type II toxin-antitoxin (TA) module (26) that is ubiquitously present in bacteria
105 and is involved in bacterial persistence and chronic infections (27). HicA is a type of
106 ribonuclease that can cause cell growth to stop when expressed without cognate antitoxin HicB.
107 So far, there is no study regarding TA systems in the genus *Fusobacterium*. We tried to explore
108 the possibility of using one of the HicA genes from fusobacterial species as a counterselection
109 marker.
110 In this study, we report the development of a HicA toxin gene-based in-frame deletion
111 system in *F. nucleatum*. We tested this system to construct two markerless in-frame deletions in
112 the fusobacterial adhesin gene *radD* and indole-producing gene *tnaA*. Following
113 counterselection, plasmid loss occurred in every colony tested, while half of the screened
114 isolates grown on plates with theophylline were in-frame deletion mutants. To our knowledge,
115 this is the first report of using a HicA as a counterselection in bacteria.
116
117 **RESULTS**
118 **A mutated HicA toxin from *F. periodonticum* is functional in *F. nucleatum***

119 In previous studies, we used the galK gene as a counterselection marker to efficiently create
120 in-frame deletion mutations in *Fusobacterium nucleatum* (17). However, the *galK*-based allelic
121 exchange system has an obvious limitation: the host cell must be *galK* minus. Without this gene,
122 bacteria were unable to utilize galactose which is crucial for survival and virulence in certain
123 conditions. This can affect the characteristics of the resulting mutant derivatives. To address this
124 issue, we in this study sought to find a new counterselection marker to replace the *galK* gene for
125 genetic manipulations in *F. nucleatum*.

126 When beginning our search for a likely candidate, we considered the toxin-antitoxin
127 modules. The toxin-antitoxin systems are widespread in bacteria and typically consist of two
128 components: a toxin that inhibits cell growth and an antitoxin that counteracts the cognate toxin
129 (28). The toxin gene *mazF* in the toxin-antitoxin MazEF modules from *E. coli* has been used for
130 counterselection in various bacteria when *mazF* expression was in highly adjustable controls,
131 most often controlled by an inducible promoter (29-34). We first attempted to use a *mazF* as a
132 counterselection marker in *F. nucleatum* but were unsuccessful. Then we switched our attention
133 to the HicA toxin gene in the HicAB toxin-antitoxin module. The HicAB system has been well
134 studied in *E. coli* (35) and *Burkholderia pseudomallei* (36). In general, the HicA toxin proteins
135 are smaller than the MazF toxin. For example, MazF in *E. coli* consists of 111 amino acids,
136 while HicA consists of 58 amino acids. MazF only works on mRNA cleavage, but HicA can
137 degrade both mRNA and transfer-messenger RNA, thereby preventing protein translations and
138 eventually leading to a growth halt. Co-expression of HicB was able to counteract HicA-induced
139 bacterial growth arrest (37, 38). Since our lab is interested in the biological roles of toxin-
140 antitoxin systems in fusobacterial species, we plan to use an endogenous HicA homolog from
141 the genus *Fusobacterium* and test if it could be employed as a counterselection marker. This
142 way, the codon-bias issue can be efficiently avoided during the ectopic expression of the
143 candidate marker gene in *F. nucleatum*, a low G+C bacterium.

144 Firstly, we identified HicA gene homologs by performing BLAST searches with the HicA
145 gene in *B. pesudomallei* (BpHicA) as a query against the genome sequence of *F.*
146 *periodonticum*, another oral bacterium. A HicA homolog was found in *F. periodonticum* and was
147 named FpHicA (see Figure 1A). It encodes a 59 amino-acid peptide by the gene of
148 *FperA3_010100004605* (https://img.jgi.doe.gov) with 61% identity and 80% similarity to BpHicA.
149 The downstream gene of *FphicA* is the *hicB*, which encodes a putative antitoxin protein for
150 neutralization of HicA toxicity (Figure 1B). Notably, the genome of *F. nucleatum* subsp.
151 *nucleatum* ATCC 23726, our genetic working strain, contains a 63 amino-acid peptide HicA
152 homolog (FnHicA) encoded by gene HMPREF0397_0209 (https://img.jgi.doe.gov). But FnHicA
153 shares a low homology with FpHicA (39% identity and 54% similarity). Suppose we use the
154 FpHicA gene as a counterselection marker in our in-frame-deletion plasmids. In that case, the
155 low sequence homology of the FpHicA gene to the FnHicA gene locus would not affect the initial
156 integration of our in-frame deletion constructs.
157
158 Next, we wanted to express the HicA gene in *F. nucleatum* ectopically and test the toxicity
159 of the FpHicA protein. To do so, the Gibson assembly cloning was performed to construct a
160 pCWU6-based (17) plasmid that expresses the HicA gene. The *rpsJ* gene promoter was proven
161 as a strong, constitutive promoter in *F. nucleatum* (6). We reasoned that the promoter of the
162 *rpsJ* gene in *F. periodonticum* (FperA3_010100002588, https://img.jgi.doe.gov/) is similar. So,
163 we used the $rpsJ_{Fp}$ promoter to drive *hicA* expression. To control the HicA expression level, a
164 well-characterized synthetic theophylline-responsive riboswitch E (39) (Figure 1C) was inserted
165 in between the $rpsJ_{fp}$ promoter and the *hicA* start codon (Figure 1E). This riboswitch E unit is
166 functional in Gram-positive and Gram-negative bacteria (39, 40). It is comprised of an aptamer
167 and a synthetic ribosome binding site (RBS). Theoretically, transcription of the riboswitch under
168 the control of the $rpsJ_{Fp}$ promoter occurs constitutively during cell growth. However, the
169 synthetic RBS located downstream of the aptamer is sequestered via pairing with the stem of

170 the riboswitch, resulting in a translational stop. The binding of ligand theophylline exposes the
171 RBS to the translation machine by altering the downstream base pairing. Consequently, the
172 *hicA* gene translation begins when the ribosome binds to the RBS (Figure 4D). We aimed to
173 obtain such plasmid with a feature of the ectopic expression of *hicA* under the control of the
174 riboswitch E element. Four positive *E. coli* clones generating by the Gibson assembly procedure
175 were randomly chosen to culture for plasmid isolation. Before the four plasmids were verified by
176 DNA sequencing, we transformed them individually into *F. nucleatum* ATCC 23726 strain by
177 electroporation. Cells were then plated out on the TSPC agar plate with thiamphenicol. The
178 colonies formed after three days of growth in an anaerobic chamber. One colony from each
179 plasmid transformation plate was picked up to grow in the TSPC medium. The growth of these
180 transformants was similar to the wild-type strain when HicA expression was not induced (data
181 not shown). Interestingly, only one transformant did not grow when 2 mM theophylline was
182 provided—the other three grew the same with or without the theophylline (Figure 2C and data
183 not shown). Later, DNA sequencing results revealed that the three plasmids are identical and all
184 contain an intact *hicA* gene. Surprisingly, the plasmid conferring cell growth arrest had a point
185 mutation in a "4A" sequence (Figure 2A). There were no errors in the promoter region,
186 riboswitch E unit, and other parts of the *hicA* gene in the four sequenced plasmids. An adenine
187 base missed in the "4A" sequence (Figure 2B), which caused a frameshift and introduced a
188 premature stop codon at codon 6. It presumably produced a five-amino acid peptide (MSSKT)
189 starting its translation from the first ATG codon when the inducer was added. By closely
190 examining the mutated *hicA* sequence, we found that the introduced stop codon TAA had one
191 nucleotide overlapping with a second ATG codon: codon 7 of the wild-type *hicA* gene (Figure
192 2A). This ATG at codon seven is postulated to allow *hicA(3A)* mRNA to restart its translation,
193 creating a shorter HicA protein lacking the first six amino acids (Figure 3B). In other words, the
194 production of short HicA protein is functional in *F. nucleatum* and ceases cell growth, but not its
195 full-length version. As the produced MSSKT peptide is a small peptide, it may act as a small-

196 peptide bacteriocin that kills or prevents bacterial growth. To exclude the possibility of the
197 MSSKT peptide acting as a bacteriocin, the gene region only synthesized with the five-amino
198 peptide was amplified from the mutated plasmid pBCG02 and re-cloned in pCWU6. Its
199 expression was under the control *rpsJ*$_{FP}$ promoter and the riboswitch E unit (pBCG04), the
200 same as those in pBCG01 and pBCG02. However, in the presence of inducers, only the
201 expression of the short peptide did not show any bacterial growth defect (Figure 2C, pBCG04).
202 The HicB protein could counteract the toxicity of mutated HicA. As the *hicB* was co-expressed
203 with mutated *hicA*, fusobacterial growth arrest was reversed (Figure 2C, pBCG03) to normal
204 level when grown on TSPA with 2 mM theophylline. We were interested in knowing if the
205 mutated HicA was functional in its native host, *F. periodonticum* as well. For that purpose, the
206 pBCG02 was transformed into *F. periodonticum* by electroporation, and one transformant was
207 further cultured and streaked on the plates. In the presence of 2 mM inducer theophylline, cell
208 growth was stopped entirely. In contrast, the cells of *F. periodonticum* with pBCG01 containing
209 the wild-type *hicA* gene showed no signs of a growth defect when HicA expression was induced
210 (Figure 2D). The real-time PCR was taken to measure the *hicA* mRNA expression level in *F.*
211 *periodonticum* cells with pBCG01 or pBCG02. The results showed that both strains expressed
212 almost the same abundance of *hicA* transcript (data not shown). In addition, we showed that
213 induction of the mutated HicA prevented cell growth of *E. coli* in an inducer dose-dependent
214 manner. 2 mM theophylline could completely abolish the growth of *E. coli* containing pBCG02
215 (Figure 2E). Together, these data suggested that the mutated HicA with 53 amino acids
216 functions as a toxin in our tested bacteria.

217 **Use of mutated HicA as a counterselection marker for in-frame deletion in *F. nucleatum***

218 The ectopic expression of HicA (3A) inhibited fusobacterial cell growth, indicating that HicA
219 (3A) might be suitable for counter-selection in *F. nucleatum*. To test this possibility, an allelic
220 exchange vector named pBCG02-Δ*radD* (Figure 3A) was constructed to delete the gene region
221 coded for the amino acids in positions between 44 and 1240 of the RadD protein. Our data

222 indicated that the RadD (44-1240) region contains a motif critical for RadD activity (unpublished
223 data). The RadD protein is a large surface adhesin that mediates *F. nucleatum's* physical
224 interactions with some oral bacteria, mostly Gram-positive, early colonizers in the human mouth
225 (5). These aggregated interactions are critical for dental plaque formation. An inverse PCR
226 linearized the pBCG02 with primer pair pCWU6-F/R to remove *repA* and ori_{FN} (Figure 3A). The
227 RepA and ori_{FN} elements are required for pCWU6-based plasmid replication in *F. nucleatum*
228 (18). Without them, the shuttle plasmid pBCG02 becomes a suicide vector with a positive
229 selection marker (*catP*) and a negative selection marker (*hicA*(3A)). We then took advantage of
230 the beauty of the Gibson assembly, which does not require restriction enzyme digestion or
231 compatible restriction sites. Instead, user-defined overlapping ends are incorporated into the
232 PCR fragments to join adjacent fragments seamlessly. The same length of upstream and
233 downstream DNA sequences flanking the region -responsible for the synthesis of the RadD (44-
234 1240)- was amplified. An overlapping PCR reaction then fused the upstream and downstream
235 fragments. Gibson assembly was used to clone the fused fragment into the linearized pBCG02
236 that lacks *repA* and ori_{FN}. The resulting in-frame deletion construct was transformed into *E. coli*
237 C2987. Positive colonies were confirmed by colony PCR using the primer pair Δ*radD*-F/R.
238 Positive colonies showed a 1.34 kb insert and were further selected for plasmid preparation and
239 sequencing. The transfer of the allelic exchange plasmid pBCG02-Δ*radD* into *F. nucleatum*
240 ATCC 23726 was traditionally performed via the electroporation procedure that our lab used
241 previously (41). The selection of recombinant vectors to integrate into the bacterial chromosome
242 was performed by thiamphenicol, a chloramphenicol derivative. One randomly selected
243 thiamphenicol-resistant integration strain was chosen for theophylline-negative selection based
244 on HicA(3A) toxicity. This strain was grown in the absence of antibiotics overnight and then
245 diluted by 1 to 1000 the following day before plating cells on the TSPC agar plates with 2 mM
246 theophylline. To estimate the frequency of plasmid excision, a plate without an inducer was
247 used to grow the un-counter-selected cells as a control. As shown in Figure 3B, the

248 theophylline-negative selection only allowed a small fraction of the cells to survive. Based on the
249 ratio of theophylline-resistant cells to total cells (cells grown on plates without selection, see
250 Figure 3B, the left plate without an inducer), we estimated that approximately 1 in 2000 cells
251 underwent a second recombination to lose the integrated plasmid. Nine randomly selected
252 theophylline-resistant colonies were confirmed for antibiotic sensitivity to screen for possible in-
253 frame deletion mutants. Next, colony PCR was used to detect their genotypes using the primer
254 pair Δ*radD*-F/R illustrated the Figure 3A. As shown in Figure 3C, five of the nine colonies
255 generated amplicons of approximately 1.4 kb, indicating an in-frame deletion. The remaining
256 four colonies generated the expected wild-type amplicons of approximately 5.0 kb. In addition,
257 the coaggregation assay was used to confirm further the three generated *radD* mutant strains.
258 As this region of RadD (44-1240) is responsible for *F. nucleatum* coaggregation with oral
259 bacterium *Actinomyces oris* (6), we expected these mutant strains to show coaggregation
260 defects. Indeed, this was the case (Figure 4D). Finally, two of the mutant strains were also
261 sequenced and found to exhibit the expected in-frame deletion that the *radD* gene only lacks in
262 the desired deletion region.
263
264 To further test this HicA(3A)-based counterselection system, we used it to make an in-
265 frame deletion of the TnaA gene (HMPREF0397_1802, https://img.jgi.doe.gov/) in *F.*
266 *nucleatum*. It has been reported that the TnaA gene encodes the enzyme tryptophanase that
267 produces indole from tryptophan in *E. coli* (42). As a signaling molecule, indole plays an
268 essential role in bacterial physiology, ecological balance, and human health (43). However, its
269 biological function in *F. nucleatum* has yet to be explored. An allelic exchange cassette carrying
270 the flanking regions of *tnaA* was generated by an overlapping PCR. The allelic exchange
271 cassette was cloned into the linearized pBCG02, in which *repA* and ori_{Fn} were omitted. The
272 generated suicide plasmid pBCG02-Δ*tnaA* (Figure 4A) was then introduced into an *F.*
273 *nucleatum* wild-type background strain by electroporation. The insertion obtained by

274 homologous recombination of the plasmid into the chromosome was selected in the presence of
275 thiamphenicol. A thiamphenicol-resistant colony was grown in TSPC without antibiotics
276 overnight. The following day, aliquots of 1000-fold diluted cultures were plated on TSPC agar
277 plates containing 2 mM theophylline. After three days, ten theophylline-resistant colonies were
278 randomly chosen to check thiamphenicol sensitivity (100% efficiency). The colony PCR was
279 then used to analyze the genotypes of the ten colonies with primer pair TnaAupF and TnaAdnR
280 (see Table 2) indicated in Figure 4A. The results revealed that half of the colonies were the
281 expected deletion mutant strains, and half were the wild-type reverent strain (Figure 4B). Lastly,
282 the *tnaA* deletion mutant was further validated by the indole assay, as a red coloration shown in
283 an oily layer at the top of the wild-type cell broth disappeared in *tnaA* mutant (Figure 4C),
284 indicating that this TnaA homolog in *F. nucleatum* is responsible for indole production.
285

286 **DISCUSSION**

287 The HicAB toxin-antitoxin system has been widely studied in bacteria. However, no HicA
288 toxin has been used for counterselection to create markerless in-frame deletion mutations. HicA
289 is a ribonuclease, and its expression prevents cell growth in many bacteria (26, 35). In this
290 study, we used a HicA gene from *F. periodonticum* and established a facile in-frame deletion
291 system in *F. nucleatum*. The success of establishing this HicA toxin for counterselection in *F.*
292 *nucleatum* has benefited from one unexpected finding. The expression of a full-length HicA
293 gene, encoded for the 59 amino-acid HicA toxin, did not induce cell death; however, when
294 inducing expression of a short form of HicA protein that lacks the first six amino acids, the cells
295 died (Figure 2C). In other words, the short version of HicA possesses a toxin activity. The
296 finding of this active form of HicA was accidental. An unexpected point mutation in *hicA*
297 occurred during plasmid constructions, allowing HicA translation to start from the second ATG,
298 codon 7, in its original version of this gene (Figure 2B). The presence of N-terminal six amino
299 acids in HicA inhibits its activity. Some proteins, like bacteriocins, must remove part of their N-

300 terminus before being active (44, 45). For toxin proteins from all studied toxin-antitoxin systems,
301 there is no such report that the removal of partial N-terminal sequences is needed for their
302 activities. *F. periodonticum* may produce a nonfunctional premature HicA protein, which then
303 requires an unknown mechanism to cleave its N-terminal partial sequence in order to be in an
304 active state. Consistently with this possibility, the *hicA* expression in the *hicB* deletion mutants
305 does not exhibit growth defects in *E. coli* (46), *Haemophilus ducreyi* (47), and *Streptococcus*
306 *mutans* (38). Another possibility is that the translation of this gene in *F. periodonticum* may start
307 from the second ATG codon -the codon 7 of the gene annotated in the genome database
308 (https://img.jgi.doe.gov)- but not the first ATG as its starting codon. All of these possibilities
309 required further studies.

310 This work aimed to find a new gene to replace *galK* as a counterselection marker to
311 generate markerless gene deletions in *F. nucleatum*. We showed that cell growth would be
312 arrested entirely when the mutated HicA was induced in the wild-type background of *F.*
313 *nucleatum* (Figure 2C). So, we attempted to use the short form of HicA as a counterselection
314 maker in allelic exchange constructs for creating in-frame-deletion mutations in *F. nucleatum*.
315 The *rpsJ* promoter is a constitutive and robust promoter in many bacteria (6, 48). We chose to
316 use the *rpsJ* promoter from *F. periodonticum* to drive the expression of the active HicA toxin.
317 Choosing the promoter from *F. periodonticum*, but not *F. nucleatum*, was to avoid the potential
318 interference to the initial integration of our constructs due to the homology of this promoter
319 fragment to the native *rpsJ* locus. A well-studied theophylline-responsive synthetic riboswitch
320 was employed to control the active HicA expression. Six synthetic theophylline-responsible
321 riboswitches were widely used in various bacteria (39, 40, 49). The riboswitch E was chosen to
322 control HicA translation because only this riboswitch works and does not have a leaking issue
323 when used in *F. nucleatum* (not published data). This theophylline-sensing riboswitch tightly
324 controls the expression of the active HicA protein. Since 2 mM of theophylline could induce
325 enough of the toxic protein to prevent cell growth, no step was carried out to optimize

326 theophylline's concentration further. With this system, we successfully created the in-frame
327 deletion for the fusobacterial adhesin protein RadD gene and the TnaA gene responsible for
328 indole production in *F. nucleatum*.

329 The HicA(3A)-based system showed a reliable and robust counterselection exactly like
330 *galK*-utilized counterselection. All colonies were thiamphenicol-sensitive after counterselection,
331 which indicated that 100% of colonies underwent loss of the integration plasmids once the
332 active HicA toxin protein was induced by 2 mM theophylline. Compared with the *galK* system,
333 the HicA(3A)-dependent counterselection has an immediate advantage: it can work in the wild-
334 type background of *F. nucleatum*. MazF has been used as a counterselection marker in other
335 Gram-positive and Gram-negative bacteria (22). As we prepared this manuscript, a MazF-
336 mediated counterselection strategy was reported in *F. nucleatum* (50). They used a tetracycline-
337 inducible system to control the MazF expression in *F. nucleatum*. The expression of MazF is
338 lethal. That allowed the counterselection in *F. nucleatum* due to MazF toxicity, and only cells
339 lacking the integrated plasmid could grow. Undoubtedly, this system is excellent and is easy to
340 use in fusobacterial genetic study. But, it has one potential problem: many strains of *F.*
341 *nucleatum* are tetracycline sensitive. We have found that even 20ng/ml tetracycline or 80ng/ml
342 anhydrotetracycline discourages the growth of *F. nucleatum* ATCC 23726, and some are even
343 more sensitive. That may limit the use of the tetracycline-induced MazF system for
344 counterselection in some strains of *F. nucleatum*. In this aspect, the theophylline-sensed
345 riboswitch is better than the tetracycline-inducible system since *F. nucleatum*'s growth is not
346 affected by the presence of theophylline, even at high concertation (data not shown).

347 The results presented in this study support the use of HicA toxin activity for negative
348 selection in *F. nucleatum*. The active HicA may work in many bacteria, as we already
349 demonstrated that the induction of this active HicA causes cell death in *F. periodonticum* and *E.*
350 *coli* (Figure 2D, 2E). As far as we know, this is the first time the HicA gene as a counterselection
351 marker for bacterial genetic studies. This same strategy is also theoretically feasible in other

352 bacteria that do not already possess an efficient negative selection system. First, it needs to
353 demonstrate HicA toxicity in the interested bacteria. This is easily done by constructing an
354 expression vector in which the combination of a strong and constitutive promoter and a
355 riboswitch unit controls the active form of HicA expression. This expression vector is then
356 transformed into the target bacterium. If the cells cease growth when the inducer is present, it
357 will suggest that HicA could be used for counterselection in this bacterium. Next, the expression
358 plasmid can be converted to a suicide vector by an inverse PCR to remove the genes required
359 for replication. This lineated vector can then serve as the cloning vector backbone for the
360 construction of an allelic exchange cassette with a Gibson assembly procedure. Finally, the
361 same two-step integration/excision strategy is employed with theophylline-based
362 counterselection. Currently, we are working on this system in *F. periodonticum* to test if it can
363 be widely applied in other fusobacterial species.
364

365 **MATERIALS AND METHODS**

366 **Bacterial strains, plasmids, and growth conditions**

367 Bacterial strains and plasmids used in this study are listed in Table 1. *F. nucleatum* and *F.*
368 *periodonticum* strains were grown in tryptic soy broth (TSB) supplemented with 1% Bacto™
369 peptone plus 0.25% freshly made cysteine (TSPC) or on TSPC agar plates in an anaerobic
370 chamber filled with 80% N_2, 10% H_2 and 10% CO_2. Hemin (5 µg/ml) and vitamin K3 (1 µg/ml)
371 were added for *F. periodonticum* growth on TSPC agar plates. *A. oris* were grown in Heart
372 Infusion Broth (HIB). *Escherichia coli* strains were grown in Luria-Bertani (LB) broth.
373 Fusobacterial transformants with pBCG01, pBCG02, pBCG03, or pBCG04 were grown
374 overnight with 5 µg/ml thiamphenicol. Overnight cultures were directly streaked on TSPC agar
375 with antibiotic selection, with or without 2 mM theophylline, after 72 h of incubation at 37°C in an
376 anaerobic chamber. 40 mM theophylline stock was prepared in a TSP medium. pREcas2 was
377 purchased from Synthetic Biology Research Center at University of Nottingham, UK. Antibiotics

378 used as needed were: chloramphenicol (15 μg ml^{-1}) and thiamphenicol (5 μg ml^{-1}). Reagents
379 were purchased from Sigma unless indicated otherwise.

380 **Plasmid construction**

381 All plasmids used in this study were constructed via Gibson assembly cloning, essentially
382 performed according to the manufacturer's instructions with NEBuilder® HIFI DNA Assembly
383 Master Mix. This method requires adjacent segments with at least 18-bp long, identical
384 sequences on the ends. These identical sequences generate via PCR with primers that contain
385 a 5' end identical to an adjacent segment and a 3' end that anneals to the gene-of-interest
386 sequence. The primers for PCR reactions were listed in Table 2.

387 pBCG01 and pBCG02– To create these plasmids, pREcas2 (40) was used as a DNA
388 template to amplify the J23119 promoter region and the riboswitch E element with primers
389 J23119-F/R. The primer pairs hicA-F/R (Table 2) were used to PCR-amplified out the *hicA* gene
390 (see gene identification no. FperA3_010100004605 in the *Fusobacterium periodonticum*
391 database at https://img.jgi.doe.gov/) with genome DNA of *Fusobacterium periodonticum* ATCC
392 33693 as a template. The two amplicons were fused via an overlapping PCR reaction, and the
393 resulting PCR product was designed as *J23119-E-hicA*. Then the fragment encompassing the
394 riboswitch E and *hicA* (E-hicA) was amplified with primers hicA($rpsJ_{FP}$)-F and hicA-R. The
395 primer pairs $PrpsJ_{FP}$-F/R were used to amplify the promoter region of the *rpsJ* gene
396 (FperA3_010100002588, https://img.jgi.doe.gov/) without its ribosome binding site ($PrpsJ_{FP}$)
397 with the genome DNA of *Fusobacterium periodonticum* ATCC 33693. The E-hicA and $PrpsJ_{FP}$
398 amplicons were cloned into SacI and HindIII-digested pCWU6 (17) by Gibson assembly and
399 transformed into *E. coli* C2987 cells, as described previously (51). Four positive clones were
400 chosen to culture for plasmid isolation, and the four plasmids were sent for sequencing. Three
401 had the wild-type *hicA* DNA sequence, but one had a point mutation at the "4A" sequence (see
402 Figure 2A, 2B). Missing an adenine base in the "4A" sequence causes a frameshift and

403 introduces a premature stop codon (PSC) at codon 6, producing a five-amino acid peptide
404 (MSSKT) starting translation from the first ATG codon. Interestingly, the stop codon TAA that
405 was introduced has one nucleotide that overlaps with the second start codon ATG (see Figure
406 2B). This second ATG codon is believed to allow the hicA(3A) mRNA to restart its translation,
407 resulting in a shorter HicA protein that is missing the first six amino acids. The plasmid that
408 contains this point mutation was named pBCG02.

409 pBCG03 –To test if the putative antitoxin HicB prevents the HicA (3A) toxicity in *F.*
410 *nucleatum*, the *hicB* gene (FperA3_010100004610, https://img.jgi.doe.gov/) was placed at
411 immediate downstream of *hicA,* and the expression of the two genes was under the control of
412 $rpsJ_{FP}$ promoter and riboswitch E unit. The fragment, including $PrpsJ_{FP}$-E-hicA, was amplified
413 with the primers $PrpsJ_{FP}$-F and hicA-R2 from pBCG02. Secondly, the primer pairs hicB-F/R
414 were used to PCR amplify the *hicB* gene. The two amplicons of $PrpsJ_{FP}$-E-hicA and hicB were
415 mixed with SacI/HindIII-cut pCWU6 in the Gibson assembly master mix solution to generate
416 pBCG03.

417 pBCG04 – With plasmid pBCG02 as a DNA template, the primer pairs $PrpsJ_{FP}$-F and
418 MSSKT-R were used to amplify the fragment encompassing $PrpsJ_{FP}$-E and *hicA* (3A) region
419 only, including the first ATG to the premature stop codon due to missing one "A" base in "4A"
420 sequence. The short *hicA* region codes a five amino-acid peptide (MSSKT, see Figure 2B).
421 This amplicon was cloned into pCWU6 precut by SacI/HindIII via Gibson assembly to generate
422 pBCG04. All produced plasmids were confirmed by sequencing and then transformed into *F.*
423 *nucleatum* ATCC 23726 or *F. periodonticum* ATCC 33693 with the electroporation procedure
424 we previously published (41).

425 **Development of a facile gene deletion method based on HicA (3A) as a counterselection**
426 **marker in *F. nucleatum***

427 To create deletion constructs of *radD* to remove the amino acids in positions between 44
428 and 1240, 1.6-kb fragments upstream and downstream of the *radD* interested region was
429 amplified by PCR using appropriate primers (Table 2). For the *tnaA* deletion plasmid, 1.6-kb
430 fragments upstream and downstream of *tnaA* were PCR amplified using tnaAupF/R and
431 tnaAdnF/R. An overlapping PCR reaction fused the upstream and downstream fragments.
432 Each fused segment was then mixed in 10 µl Gibson assembly master mix solution with an
433 equal amount of the pBCG02 vector backbone in which the *repA* and ori_{Fn} element were
434 removed by inverse PCR with primer pairs pCWU6-F/R (see Figure 3A). A 2x hot-start PCR
435 master mix from Takara was used for high-fidelity PCR amplification of the pBCG02 backbone.
436 The resulting plasmids pBCG02-Δ*radD* and pBCG02-Δ*tnaA* were further confirmed by DNA
437 sequencing and transformed into *F. nucleatum* ATCC 23726 by electroporation, respectively.

438 Plasmid insertion into the bacterial chromosome by homologous recombination was
439 selected by growth in the presence of 5 µg/ml thiamphenicol at 37°C. A 5 µg/ml thiamphenicol-
440 resistant colony was inoculated overnight in TSPC without antibiotics. The following day, a 100
441 µl aliquot of 1,000-fold diluted cultures was plated on TSPC agar plates containing two mM
442 inducer theophylline to select for cells in which the plasmid had been excised and lost. In the
443 presence of the inducer, cells in which the plasmid is still present produce HicA(3A) toxin at
444 toxic levels and do not form colonies. Growing 9~10 colonies were restreaked on TSPC plates,
445 checked for thiamphenicol sensitivity (100% efficiency), and screened by PCR amplification for
446 the presence of the expected deletion in *radD* or *tnaA*.

447 **Bacterial co-aggregation**

448 Co-aggregation assays were performed with wild-type and Δ*radD* strains of *Fusobacterium*
449 *nucleatum* and *Actinomyces oris* MG-1 as previously described (17). Briefly, stationary-phase
450 cultures of bacterial strains were grown in TSPC or heart infusion broth (for MG-1) harvested by
451 centrifugation, washed in coaggregation buffer (52), and suspended to an equal cell density of

452 approximately 2 x 10^9 ml^{-1} based upon OD_{600} values. For co-aggregation, 0.20 ml aliquots of
453 *Actinomyces* and fusobacterial cell suspensions were mixed in a 24-well plate for a few minutes
454 on a rotator shaker, and images were taken.

455 **Indole assay**

456 Fusobacterial wild-type and Δ*tnaA* deletion strains were individually inoculated into a test
457 tube with 5ml TSPC medium. After incubation at 37°C for 48 hours, a 200 µl of Kovacs's
458 reagent was added to each tube without shaking. Observe for the presence or absence of a
459 cherry-red ring. A positive indole test is indicated by the formation of a pink to red color ("cherry-
460 red ring") in the reagent layer on top of the medium within seconds of adding the reagent. A
461 negative result appears yellow. The photo was taken in 10 minutes.

462 **AUTHOR CONTRIBUTIONS**

463 C.W. conceived and designed all experiments. B.G. and P.Z. performed all experiments. B.G.,
464 P.Z., and C. W. analyzed data. C.W. wrote the manuscript with contribution and approval from
465 all authors.

466 **DATA AVAILABILITY STATEMENT**

467 Materials are available upon reasonable request with a material transfer agreement with
468 UTHealth for bacterial strains or plasmids. pBCG01 plasmid sequence and map can be
469 accessed on a Benchling link at https://benchling.com/s/seq-VuTCpImziZSBrxT6otvO?m=slm-
470 jUtGU7tIsA1ZnPAgUH1f

471 **ACKNWLEDGMENTS**

472 This work was supported by a National Institute of Dental and Craniofacial Research (NIDCR)
473 grant (DE030895) to C.W.

474 **REFERENCES**

475

476 1. B. J. Paster *et al.*, Bacterial diversity in human subgingival plaque. *Journal of*
477 *bacteriology* **183**, 3770-3783 (2001).

478 2. A. Bolstad, H. B. Jensen, V. Bakken, Taxonomy, biology, and periodontal aspects of
479 Fusobacterium nucleatum. *Clinical microbiology reviews* **9**, 55-71 (1996).

480 3. Y. W. Han *et al.*, Identification and characterization of a novel adhesin unique to oral
481 fusobacteria. *Journal of bacteriology* **187**, 5330-5340 (2005).

482 4. Y. Fardini *et al.*, Fusobacterium nucleatum adhesin FadA binds vascular endothelial
483 cadherin and alters endothelial integrity. *Molecular microbiology* **82**, 1468-1480 (2011).

484 5. C. W. Kaplan, R. Lux, S. K. Haake, W. Shi, The Fusobacterium nucleatum outer
485 membrane protein RadD is an arginine-inhibitable adhesin required for inter-species
486 adherence and the structured architecture of multispecies biofilm. *Molecular*
487 *microbiology* **71**, 35-47 (2009).

488 6. C. Wu *et al.*, Genetic and molecular determinants of polymicrobial interactions in
489 Fusobacterium nucleatum. *Proc Natl Acad Sci U S A* **118** (2021).

490 7. J. Abed *et al.*, Fap2 mediates Fusobacterium nucleatum colorectal adenocarcinoma
491 enrichment by binding to tumor-expressed Gal-GalNAc. *Cell host & microbe* **20**, 215-225
492 (2016).

493 8. L. Parhi *et al.*, Placental colonization by Fusobacterium nucleatum is mediated by
494 binding of the Fap2 lectin to placentally displayed Gal-GalNAc. *Cell Rep* **38**, 110537
495 (2022).

496 9. D. Polak, L. Shapira, E. I. Weiss, Y. Houri-Haddad, The role of coaggregation between
497 Porphyromonas gingivalis and Fusobacterium nucleatum on the host response to mixed
498 infection. *Journal of clinical periodontology* **39**, 617-625 (2012).

499 10. Y. Zhang, W. Shi, Y. Song, J. Wang, Metatranscriptomic analysis of an in vitro biofilm
500 model reveals strain-specific interactions among multiple bacterial species. *J Oral*
501 *Microbiol* **11**, 1599670 (2019).
502 11. E. L. Vander Haar, J. So, C. Gyamfi-Bannerman, Y. W. Han, Fusobacterium nucleatum
503 and adverse pregnancy outcomes: epidemiological and mechanistic evidence. *Anaerobe*
504 **50**, 55-59 (2018).
505 12. S. Gauthier *et al.*, The origin of Fusobacterium nucleatum involved in intra-amniotic
506 infection and preterm birth. *The journal of Maternal-fetal & Neonatal Medicine* **24**, 1329-
507 1332 (2011).
508 13. T. Yu *et al.*, Fusobacterium nucleatum promotes chemoresistance to colorectal cancer
509 by modulating autophagy. *Cell* **170**, 548-563. e516 (2017).
510 14. L. Flanagan *et al.*, Fusobacterium nucleatum associates with stages of colorectal
511 neoplasia development, colorectal cancer and disease outcome. *European journal of*
512 *clinical microbiology & infectious diseases* **33**, 1381-1390 (2014).
513 15. M. R. Rubinstein *et al.*, Fusobacterium nucleatum promotes colorectal carcinogenesis by
514 modulating E-cadherin/β-catenin signaling via its FadA adhesin. *Cell host & microbe* **14**,
515 195-206 (2013).
516 16. C. A. Brennan, W. S. Garrett, Fusobacterium nucleatum—symbiont, opportunist and
517 oncobacterium. *Nature Reviews Microbiology* **17**, 156-166 (2019).
518 17. C. Wu *et al.*, Forward Genetic Dissection of Biofilm Development by Fusobacterium
519 nucleatum: Novel Functions of Cell Division Proteins FtsX and EnvC. *mBio* **9** (2018).
520 18. S. K. Haake, S. Yoder, S. H. Gerardo, Efficient gene transfer and targeted mutagenesis
521 in Fusobacterium nucleatum. *Plasmid* **55**, 27-38 (2006).
522 19. M. A. Casasanta *et al.*, Fusobacterium nucleatum host-cell binding and invasion induces
523 IL-8 and CXCL1 secretion that drives colorectal cancer cell migration. *Science signaling*
524 **13**, eaba9157 (2020).

525 20. Q. Meng *et al.*, Fusobacterium nucleatum secretes amyloid-like FadA to enhance
526 pathogenicity. *EMBO reports* **22**, e52891 (2021).
527 21. A. Ikegami, P. Chung, Y. W. Han, Complementation of the fadA mutation in
528 Fusobacterium nucleatum demonstrates that the surface-exposed adhesin promotes
529 cellular invasion and placental colonization. *Infect Immun* **77**, 3075-3079 (2009).
530 22. J.-M. Reyrat, V. Pelicic, B. Gicquel, R. Rappuoli, Counterselectable markers: untapped
531 tools for bacterial genetics and pathogenesis. *Infection and immunity* **66**, 4011-4017
532 (1998).
533 23. A. Umaña *et al.*, Enhanced Fusobacterium nucleatum Genetics Using Host DNA
534 Methyltransferases To Bypass Restriction-Modification Systems. *Journal of Bacteriology*
535 **204**, e00279-00222 (2022).
536 24. K. Vaillancourt *et al.*, Role of galK and galM in galactose metabolism by Streptococcus
537 thermophilus. *Applied and environmental microbiology* **74**, 1264-1267 (2008).
538 25. A. R. Neves *et al.*, Towards enhanced galactose utilization by Lactococcus lactis.
539 *Applied and environmental microbiology* **76**, 7048-7060 (2010).
540 26. K. S. Makarova, N. V. Grishin, E. V. Koonin, The HicAB cassette, a putative novel, RNA-
541 targeting toxin-antitoxin system in archaea and bacteria. *Bioinformatics* **22**, 2581-2584
542 (2006).
543 27. G. Singh, M. Yadav, C. Ghosh, J. S. Rathore, Bacterial toxin-antitoxin modules:
544 classification, functions, and association with persistence. *Current Research in Microbial*
545 *Sciences* **2**, 100047 (2021).
546 28. D. Jurėnas, N. Fraikin, F. Goormaghtigh, L. Van Melderen, Biology and evolution of
547 bacterial toxin–antitoxin systems. *Nature Reviews Microbiology* **20**, 335-350 (2022).
548 29. Y. Shi, H. Dong, D. Zhang, Application Progress of mazF Gene in Genetic Modification
549 System. *Biotechnology Bulletin*, 48 (2014).

550 30. T. Morimoto, K. Ara, K. Ozaki, N. Ogasawara, A new simple method to introduce
551 marker-free deletions in the Bacillus subtilis genome. *Genes & genetic systems* **84**, 315-
552 318 (2009).
553 31. Y. E. Cheah, S. C. Albers, C. A. Peebles, A novel counter-selection method for
554 markerless genetic modification in Synechocystis sp. PCC 6803. *Biotechnology progress*
555 **29**, 23-30 (2013).
556 32. W. F. Van Zyl, L. M. Dicks, S. M. Deane, Development of a novel selection/counter-
557 selection system for chromosomal gene integrations and deletions in lactic acid bacteria.
558 *BMC molecular biology* **20**, 1-16 (2019).
559 33. L. Chen, H. Liu, L. Wang, X. Tan, S. Yang, Synthetic counter-selection markers and their
560 application in genetic modification of Synechococcus elongatus UTEX2973. *Applied*
561 *Microbiology and Biotechnology* **105**, 5077-5086 (2021).
562 34. Z. Lin *et al.*, A versatile mini-mazF-cassette for marker-free targeted genetic modification
563 in Bacillus subtilis. *Journal of microbiological methods* **95**, 207-214 (2013).
564 35. M. G. Jørgensen, D. P. Pandey, M. Jaskolska, K. Gerdes, HicA of Escherichia coli
565 defines a novel family of translation-independent mRNA interferases in bacteria and
566 archaea. *Journal of bacteriology* **191**, 1191-1199 (2009).
567 36. A. Butt *et al.*, The HicA toxin from Burkholderia pseudomallei has a role in persister cell
568 formation. *Biochemical Journal* **459**, 333-344 (2014).
569 37. A. T. Butt, Identification and characterisation of toxin-antitoxin systems (TA) in
570 Burkholderia pseudomallei. (2013).
571 38. Z. Xie, F. Qi, J. Merritt, Development of a tunable wide-range gene induction system
572 useful for the study of streptococcal toxin-antitoxin systems. *Applied and environmental*
573 *microbiology* **79**, 6375-6384 (2013).
574 39. S. Topp *et al.*, Synthetic riboswitches that induce gene expression in diverse bacterial
575 species. *Applied and environmental microbiology* **76**, 7881-7884 (2010).

576 40. I. C. Canadas, D. Groothuis, M. Zygouropoulou, R. Rodrigues, N. P. Minton, RiboCas: A
577 Universal CRISPR-Based Editing Tool for Clostridium. *ACS Synth Biol* **8**, 1379-1390
578 (2019).
579 41. E. A. Peluso, M. Scheible, H. Ton-That, C. Wu, Genetic Manipulation and Virulence
580 Assessment of Fusobacterium nucleatum. *Curr Protoc Microbiol* **57**, e104 (2020).
581 42. G. Li, K. D. Young, Indole production by the tryptophanase TnaA in Escherichia coli is
582 determined by the amount of exogenous tryptophan. *Microbiology* **159**, 402-410 (2013).
583 43. J.-H. Lee, J. Lee, Indole as an intercellular signal in microbial communities. *FEMS*
584 *microbiology reviews* **34**, 426-444 (2010).
585 44. M. Zimina *et al.*, Overview of global trends in classification, methods of preparation and
586 application of bacteriocins. *Antibiotics* **9**, 553 (2020).
587 45. A. Darbandi *et al.*, Bacteriocins: Properties and potential use as antimicrobials. *Journal*
588 *of Clinical Laboratory Analysis* **36**, e24093 (2022).
589 46. J. E. Button, T. J. Silhavy, N. Ruiz, A suppressor of cell death caused by the loss of σE
590 downregulates extracytoplasmic stress responses and outer membrane vesicle
591 production in Escherichia coli. *Journal of bacteriology* **189**, 1523-1530 (2007).
592 47. A. Yeung, D. W. Cameron, M. Desjardins, B. C. Lee, Use of signature-tagged
593 mutagenesis to identify virulence determinants in Haemophilus ducreyi responsible for
594 ulcer formation. *Journal of microbiological methods* **84**, 290-298 (2011).
595 48. C. Wu, H. Ton-That, Allelic exchange in Actinomyces oris with mCherry fluorescence
596 counterselection. *Applied and Environmental Microbiology* **76**, 5987-5989 (2010).
597 49. C. Wu *et al.*, Lethality of sortase depletion in A ctinomyces oris caused by excessive
598 membrane accumulation of a surface glycoprotein. *Molecular microbiology* **94**, 1227-
599 1241 (2014).

600 50. F. Ponath, Y. Zhu, V. Cosi, J. Vogel, Expanding the genetic toolkit helps dissect a global
601 stress response in the early-branching species Fusobacterium nucleatum. *Proceedings*
602 *of the National Academy of Sciences* **119**, e2201460119 (2022).
603 51. D. G. Gibson *et al.*, Enzymatic assembly of DNA molecules up to several hundred
604 kilobases. *Nature methods* **6**, 343-345 (2009).
605 52. J. O. Cisar, P. Kolenbrander, F. McIntire, Specificity of coaggregation reactions between
606 human oral streptococci and strains of Actinomyces viscosus or Actinomyces naeslundii.
607 *Infection and immunity* **24**, 742-752 (1979).
608

609 **Table 1:** Bacterial strains and plasmids used

Strain & Plasmid	Description	Reference
Strains		
F. periodonticum 33693	Parental strain	This study
F. nucleatum 23726	Parental strain	(5)
F. nucleatum BG01	Δ *radD*; an isogenic derivative of 23726	This study
F. nucleatum ZP01	Δ*tnaA*; an isogenic derivative of 23726	This study
A. oris MG1	Wild Type strain	(48)
E. coli C2987	Cloning host	From NEB
Plasmids		
pCWU6	*E. coli*/*Fusobacterium* shuttle vector, chloramphenicol /thiamphenicol resistance; cm^R/$thia^R$	(18)
pRECas2	The J23119 promoter incorporating the riboswitch element E controls Cas9 expression	(40)
pBCG01	pCWU6 expressing wild-type *hicA* gene [*hicA*(4A)] from *F. periodonticum* 33693 under the control of the $rpsJ_{FP}$ promoter and its ribosome binding site was replaced by a riboswitch element E from pRECas2	This study
pBCG02	Derivative of pBCG01 expressing *hicA* with a point mutation [*hicA*(3A)]. The *hicA*(3A) mRNA is translated from the initiation site met-7, giving a shorter protein lacking the first six amino acids.	This study

pBCG03	Derivative of pBCG02 co-expressing *hicA*(3A) and *hicB,* the cognate hicA anti-toxin gene	This study
pBCG04	Derivative of pBCG02 expressing the five amino acids peptide (MSSKT) alone	This study
pBCG02-Δ*radD*	Derivative of pBCG02 lacking *repA* and ori_{Fn}, deletion vector of *radD Δ41-1240*	This study
pBCG02-Δ*tnaA*	Derivative of pBCG02 lacking *repA* and ori_{Fn}, deletion vector of *tnaA*	This study

610
611
612
613 **Table 2:** Primers used in this study

Primer	Sequence[(a)]	Used for
J23119-F	GAAACAGCTATGACATGATTACGAATTCGAGCT CTGAGCTAGCTGTCAAACTGGCCGTCG	pBCG01
J23119-R	AGTAATTTCATTAGGTCTTTTGAGCTCATCTTGTTGTTAC CTCCTTAGCAGG	pBCG01
hicA-F	GCTAAGGAGGTAACAACAAGATGAGCTCAA AAGACCTAAT GAAATTACT	pBCG01
hiA-R	GTATAAATGTTAGTGATGATTATAAAA ATTAAAAGTATGAGGAGAACAAGCAAG	pBCG01
$PrpsJ_{FP}$-F	GAAACAGCTATGACATGATTACGAATTCGAGCT AGCACCAGGT TTAGGGGCTG CTATAG	pBCG01
$PrpsJ_{FP}$-R	GGCATCAAGACGATGCTGGTATCACCGGTTTAAATTAA CTACATAAGATAATTCTTATG	pBCG01
hicA($rpsJ_{FP}$)-F	GAATTATCTTATGTAGTTAATTTAAA CCGGTGATACCAGCATCGTCTTGATGCCCTTG	pBCG01
hicA-R2	AAGTATGAGGAGAACAAGCAAGGCATTAAAGCCCTGCT TGCCTG	pBCG01
hicB-F	CAGGCAAGCAGGGCTTTAATGCCTTGCTT GTTCTCCTCA TACTT	pBCG03
hicB-R	GTATAAATGTTAGTGATGATTATAAAA TTATTTTTCAATTCCTAATTCTTTT	pBCG03
MSSKT-R	GTATAAATGTTAGTGATGATTATAAAA TTAGGTCTTTGAGCTCATCTTGTTG	pBCG04
pCWU6-F	GTCCTAGAACTAGTGAAATTTCCG	Remove *repA* and ori_{Fn} from pBCG02
pCWU6-R	GTAGCTTCCATACATATCACACTC	Remove *repA*
TnaAupF	GAGTGTGATATGTATGGAAGCTACAGTAATATTG TTTGATGAAATTGAAAAGG	and ori_{Fn} from pBCG02 pBCG02-Δ*tnaA*
TnaAupR	TCTGCTTGTTGTTCAGGAGTTTCATCACCTAGGAACATA GCTGACCATTG	pBCG02-Δ*tnaA*
TnaAdnF	GCTATGTTCCTAGGTGATGAAACTCCTGAACAACAAGC AGAAGTTGCAAATG	pBCG02-Δ*tnaA*

TnaAdnR	CGGAAATTTCACTAGTTCTAGGACAGCAGCAA GCAATGCTCC AAGTGGACAA ATATATATAG	pBCG02-Δ*tnaA*
RadDupF	GAGTGTGATATGTATGGAAGCTACATAAATTTAATTTAA CTTATTAATTATAAGG	pBCG02-Δ*radD*
RadDupR	GCATCCTTACCTGACATTTTTACTGCTTCATCTGCATAA GAAAAACCACCATTAAT	pBCG02-Δ*radD*
RadDdnF	GATGAAGCAGTAAAAATGTCAGGTAAGGATGC TATTGGTATTT	pBCG02-Δ*radD*
RadDdnR	CGGAAATTTCACTAGTTCTAGGACTCCTGATTCATTTAT TGCTTCACCATCTACT	pBCG02-Δ*radD*
Δ*radD*-F	GAGTTTCAGATGAAATGAATGCCCTACAAG	Confirm *radD* deletion
Δ*radD*-R	CTGCAGTAGTTGCTCCACCTTTTACAGCTG	Confirm *radD* deletion

[(a)]Underlined are primer sequence specific to the ends of the corresponding assembly

FIGURE LEGENDS

Figure 1: Construction of *E. coli*/*Fusobacterium* shuttle plasmid pBCG01 expressing putative HicA toxin under the control of riboswitch E-based inducible system. (A) Protein alignment of toxin HicA from *Burkholderia pseudomallei* (BpHicA) with HicA encoded by *FperA3_010100004605* (https://img.jgi.doe.gov) in *Fusobacterium periodonticum* ATCC 33693 (FpHicA) using ClustalW program. **(B)** Genetic organization of the *hicA*-*hicB* toxin-antitoxin pair in *F. periodonticum* and the whole DNA sequence of the HicA gene. **(C)** The mRNA sequence of the riboswitch E is shown with an aptamer sequence emboldened, ribosome binding site (RBS) sequence highlighted, and start codon red colored. **(D)** Schematic diagrams of a functional model of the theophylline responsive riboswitch. Without theophylline, the riboswitch forms a stem-loop structure that conceals the RBS in the mRNA transcript. The riboswitch alters its confirmation when theophylline binds to the aptamer, resulting in the release of the RBS and the initiation of translation of *hicA*. **(E)** *E. coli*/*Fusobacterium* shuttle plasmid pBCG01 containing

635 *hicA* gene under the control of *rpsJ* promoter from *F. periodonticum*. The RBS in the *rpsJ*
636 promoter region was replaced by the riboswitch E element. ColE1 RNA II origin (ori_{Ec}), the pFN1
637 ori (ori_{Fn}), *repA* gene, and *catP* gene were indicated. The ori_{Ec} allows replication of the shuttle
638 plasmid in *E. coli*, and the plasmid replicates in *F. nucleatum,* requiring the ori_{Fn} and *repA*.

639 **Figure 2: A shorter HicA protein that lacks the first six amino acids is functional in**
640 ***Fusobacterium nucleatum* and other bacteria (A)** The plasmid pBCG01 contains an intact
641 *hicA* gene, indicating the presence of a four consecutive adenine base sequence (4A) after the
642 start codon (red colored). The wild-type *hicA* encodes a 59-amino acid protein. **(B)** An adenine
643 base was missing from the 4A sequence resulting in the *hicA* gene (3A) during construction of
644 pBCG01. We later named that mutated construct as pBCG02. This point mutation causes a
645 frameshift resulting in a premature stop codon (TAA, underlined) at codon six and generates
646 five amino acids peptide (MSSKT). The *hicA* (3A) mRNA then restarts its translation from the
647 new initiation site (ATG, emboldened), giving a shorter HicA protein lacking the first six amino
648 acids. **(C)** Growth of *F. nucleatum* strain 23726 harboring the plasmid construct pGCG01,
649 pBCG02, pBCG03, or pBCG04 on TSPC agar plates supplemented with thiamphenicol plus 0
650 (non-induced) or 2mM (induced) theophylline and incubated at 37°C in an anaerobic chamber
651 for two days. Schematic representations of the constructs are shown in the left diagram. **(D)**
652 Growth of *F. periodonticum* containing the plasmid pBCG01 or pBCG02 on TSPC agar plates
653 under the uninduced or induced condition with theophylline after two days of growth in an
654 anaerobic chamber. **(E)** Overnight E. *coli* containing pBCG02 was diluted by 1:1000 and
655 aliquoted into three tubes with 6 ml LB broth plus an indicated concertation of theophylline after
656 18 hours of growth with shaking (200 rpm) at 37°C. These experiments were performed more
657 than three times, and a representative result was presented.

658 **Figure 3: Applying HicA (3A) as a counter-selectable marker for gene deletion in *F.***
659 ***nucleatum*. (A)** Graphic representation of producing the non-replicative vector backbone
660 pBCG02-Δ used to generate unmarked, in-frame gene deletions in *F. nucleatum*. The primer

661 pairs (pCWU6-F/R, indicated by short arrows) were used to perform reverse PCR to remove the
662 region, including the ori_{Fn} and *repA*. The *radABCD* operon is shown. Approximately 1.6 kb
663 fragments homologous to the upstream (blue) and downstream (green) regions of the designed
664 deletion region in *radD* were amplified by PCR. They have ligated adjacently on the vector
665 backbone pBCG02-Δ via the Gibson assembly procedure (see details in context). The resulting
666 plasmid pBCG02-Δ*radD* was used to generate an unmarked *radD* deletion mutant in the wild-
667 type background. **(B)** TSPC agar plate representative of the counterselection effect by
668 HicA(3A) toxin expression in *F. nucleatum*. A 100 µl aliquot of 1,000-fold diluted overnight
669 culture for pBCG02- pBCG02-Δ*radD* integrated strain was plated on TSPC agar plates
670 containing 0 or 2 mM inducer theophylline to select for cells in which the plasmid had been
671 excised and lost. **(C)** The screen of *radD* deletion mutants by colony PCR with the primer pairs
672 Δ*radD*-F/R. Lane 1-9, 10 µl of PCR products of nine colonies randomly selected from the TSPC
673 plate. Five of the nine chosen random colonies were deletion mutants, while four reverted to
674 wild-type during the second recombination event. Bands of approximately 1.4 kb indicate *radD*
675 deletion, whereas bands of about 5.0 kb indicate a wild-type (WT) genotype. **(D)** *F. nucleatum*
676 wild-type and three *radD* mutant strains were examined for coaggregation with *Actinomyces oris*
677 MG-1.

678 **Figure 4: Deletion of indole-producing gene *tnaA* in F. nucleatum as HicA (3A) as a**
679 **counter-selectable marker. (A)** Schematic drawing of pBCG02-Δ*tnaA* for deletion
680 tryptophanase TnaA gene. Approximately 1.6-kb fragments homologous to the upstream (blue)
681 and downstream (green) regions of the TnaA gene were ligated adjacently on the vector
682 backbone pBCG02-Δ via Gibson assembly procedure to create the vector pBCG02-Δ*tnaA*. The
683 primer pairs for colony PCR to screen Δ*tnaA* mutant strains were indicated by small arrows. **(B)**
684 The genotype of *tnaA* mutant strains following HicA (3A) counterselection. Bands of
685 approximately 3.2 kb indicate a *tnaA* deletion, whereas bands of about 5.0 kb indicate a wild-

686 type genotype. “WT” represents the parent wild-type, ATCC23726. **(C)** *F. nucleatum* wild-type
687 and a *TnaA* mutant strain were examined for indole production. Indole production was
688 demonstrated by adding Kovac’s reagent (200 µl), which acts with the indole giving a red color
689 in 5ml fusobacterial cultures.
690
691

A

```
BpHicA     MNSSKLIRMLEEDGWRLVRVTGSAHHFKHPKKPGLVTVPHPKKDLPIGTVKSIQKSAGL
           |.|..|:::|..||| | ||.||  ||||..|.|||||||||:||||: ||.|| : |||
FpHicA     MSSKDLMKLLKKDGWYLDRVNGSHYHFKHKSKKGLVTVPHPRKDLPLKTVESIFRQAGL
```

B

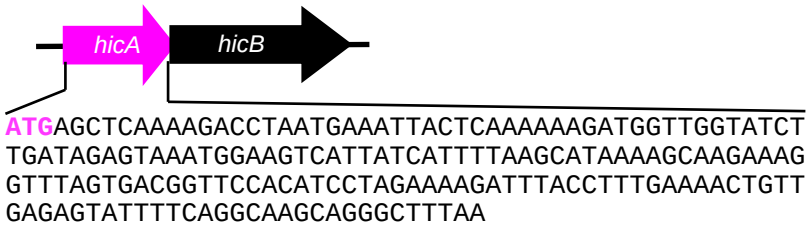

C Riboswitch E sequence

CC**GGUGAUACCAGCAUCGUCUUGAUGCCCUUGGCAGCACCCUGCUAAGCAAGGAGGUAACAACAAGAUG**

RBS

D

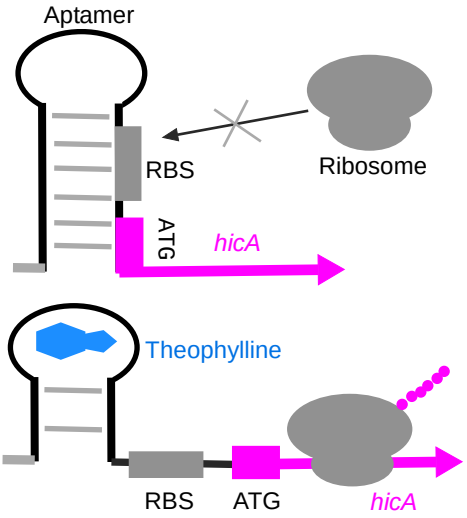

E

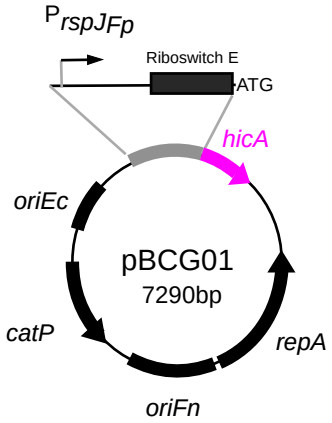

Figure 1: Bibek et al.

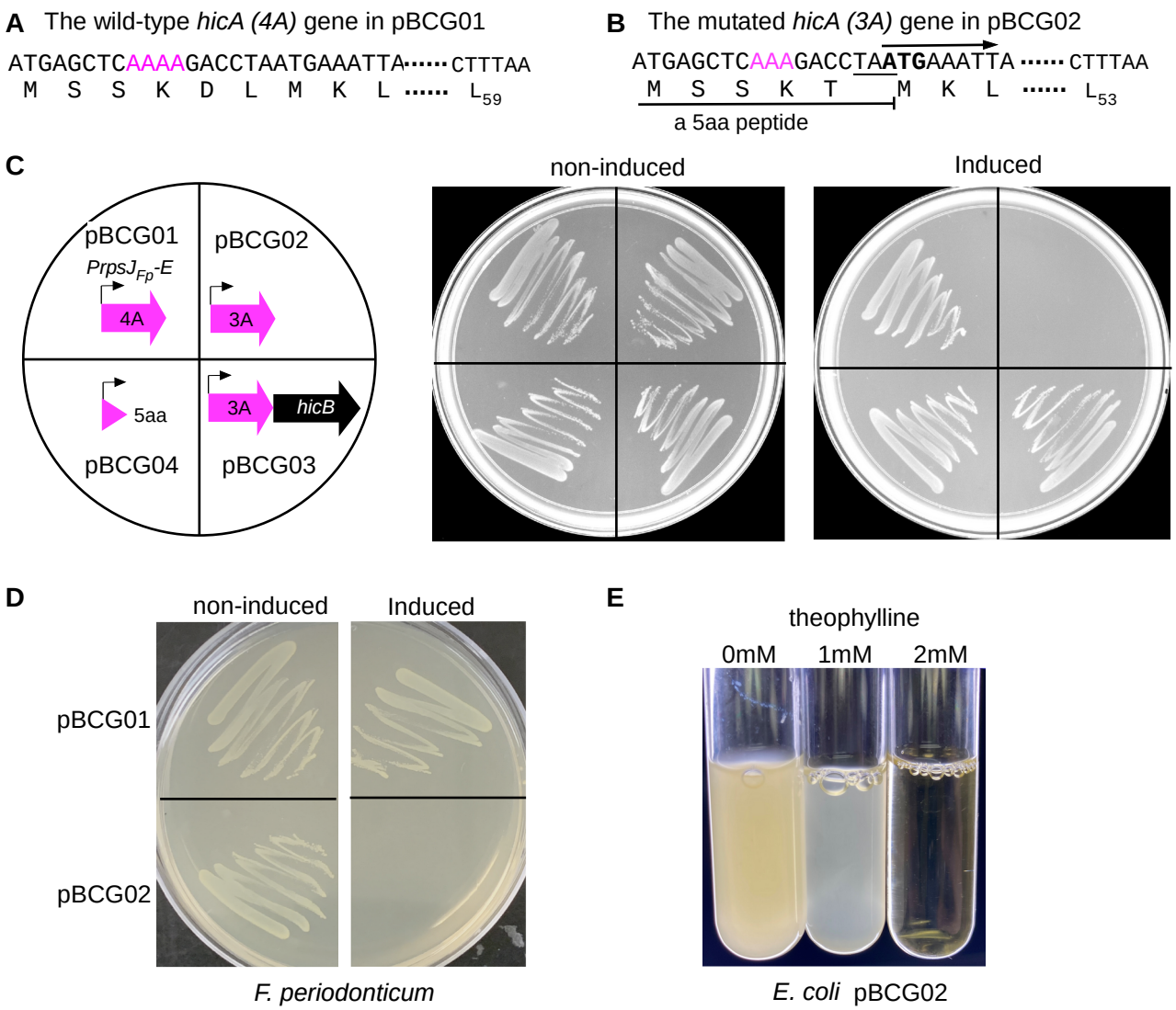

Figure 2: Bibek et al.

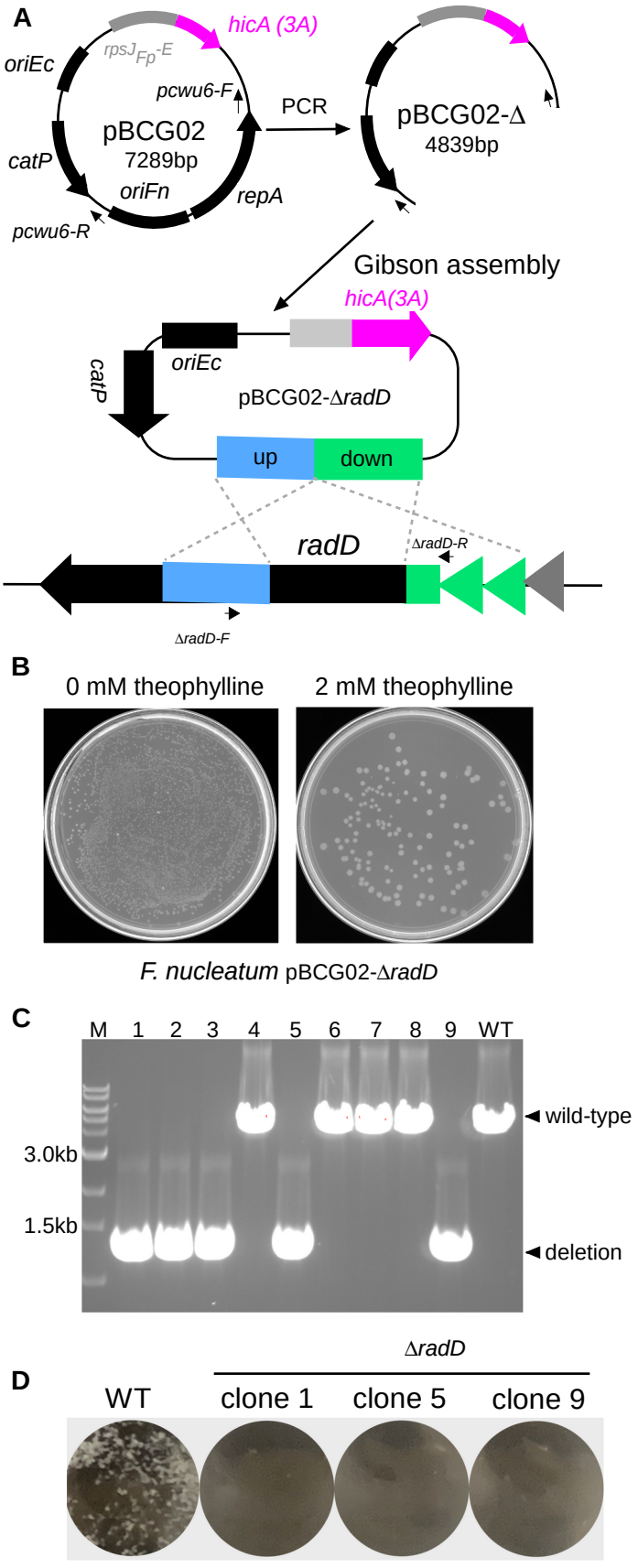

Figure 3: Bibek et al.

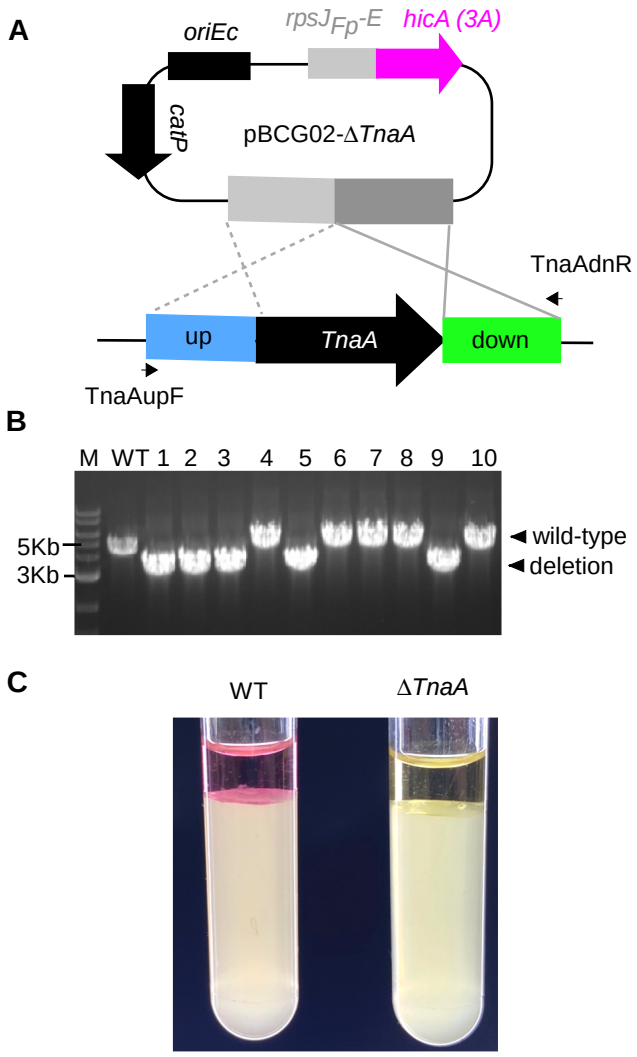

Figure 4: Bibek et al.